

Article

Preparation and Spectroscopic Characterization of Ternary Inclusion Complexes of Ascorbyl Palmitate and Urea with γ -Cyclodextrin

Yutaka Inoue ^{1,*}, Ayumi Nanri ¹, Florencio Jr. Arce ², Gerard Lee See ², Takashi Tanikawa ¹, Takami Yokogawa ³ and Masashi Kitamura ³

¹ Laboratory of Nutri-Pharmacotherapeutics Management, Faculty of Pharmacy and Pharmaceutical Sciences, Josai University, 1-1, Keyakidai, Sakado 350-0295, Saitama, Japan

² Pharmaceutical Research and Drug Development Laboratories, Department of Pharmacy, School of Health Care Professions, University of San Carlos, Cebu City 6000, Philippines

³ Laboratory of Pharmacognosy, Faculty of Pharmacy and Pharmaceutical Sciences, Josai University, 1-1, Keyakidai, Sakado 350-0295, Saitama, Japan

* Correspondence: yinoue@josai.ac.jp; Tel.: +81-49-271-7980

Abstract: A three-component inclusion complex of ascorbyl palmitate (ASCP), urea (UR), and γ -cyclodextrin (γ CD) with a molar ratio of 1/12 has been prepared for the first time using the evaporation method (EVP method) and the grinding and mixing method (GM method). Also, we investigated changes in the physicochemical properties of the three-component complexes. The powder X-ray diffraction (PXRD) measurements showed ASCP, UR, and γ CD characteristic peaks in the physical mixture (PM) (AU (ASCP/UR = 1/12)/ γ CD = 1/2). In GM (AU (ASCP/UR = 1/12)/ γ CD = 1/1), new diffraction peaks were observed around $2\theta = 7.5^\circ$ and 16.6° , while characteristic peaks derived from EVP (ASCP/UR = 1/12) were observed at $2\theta = 23.4^\circ$ and 24.9° . On the other hand, new diffraction peaks at $2\theta = 7.4^\circ$ and 16.6° were observed in GM (1/2). In the differential scanning calorimeter (DSC) measurement, an endothermic peak at around 83°C was observed in the GM (1/1) sample, which is thought to originate from the phase transition of urea from the hexagonal to the tetragonal form. An endothermic peak around 113.9°C was also observed for EVP (ASCP/UR = 1/12). However, no characteristic phase transition-derived peak or EVP (ASCP/UR = 1/12)-derived endothermic peak was observed in GM (1/2). Near infrared (NIR) spectroscopy of GM (1/2) showed no shift in the peak derived from the CH group of ASCP. The peaks derived from the NH group of UR shifted to the high and low wavenumber sides at 5032 cm^{-1} and 5108 cm^{-1} in EVP (ASCP/UR = 1/12). The peak derived from the OH group of γ CD shifted, and the peak derived from the OH group of ASCP broadened at GM (1/2). These results suggest that AU (ASCP/UR = 1/12)/ γ CD prepared by the mixed grinding method formed inclusion complexes at the molar ratio (1/2).



Citation: Inoue, Y.; Nanri, A.; Arce, F.J.; See, G.L.; Tanikawa, T.; Yokogawa, T.; Kitamura, M. Preparation and Spectroscopic Characterization of Ternary Inclusion Complexes of Ascorbyl Palmitate and Urea with γ -Cyclodextrin. *ChemEngineering* **2023**, *7*, 29. <https://doi.org/10.3390/chemengineering7020029>

Academic Editor: Alirio E. Rodrigues

Received: 2 March 2023

Revised: 25 March 2023

Accepted: 27 March 2023

Published: 29 March 2023



Copyright: © 2023 by the authors. Licensee MDPI, Basel, Switzerland. This article is an open access article distributed under the terms and conditions of the Creative Commons Attribution (CC BY) license (<https://creativecommons.org/licenses/by/4.0/>).

Keywords: ascorbyl palmitate; urea; γ -cyclodextrin; inclusion complexes; complexation; formulation

1. Introduction

Ascorbic acid (AA), a type of water-soluble vitamin with a lactone ring in its structure, is a potent antioxidant molecule. In vivo, AA eliminates reactive oxygen species through electron transfer and promotes collagen production by activating transcription factors. It is widely used as a dietary supplement and in health foods, cosmetics, and other products [1–3]. However, ascorbic acid alone is easily oxidized in aqueous solutions and has low stability under conditions of light, heat, and acids [4]. Recently, various ascorbic acid derivatives have been synthesized to improve the stability of ascorbic acid [5,6]. One such derivative of ascorbic acid is ascorbyl palmitate (ASCP), which is an ester formed between AA and palmitic acid. ASCP has high fat solubility and improved stability against heat

and light. It is also used in cosmetics for topical applications because of its antioxidant properties [7].

Urea (UR) is widely used as a main ingredient in pharmaceuticals and cosmetics as a humectant and skin penetration enhancer due to its moisturizing ability, stratum corneum hydrating properties, and keratin cleavage properties [8]. UR is characterized as hydrophilic and dissolves organic compounds in water at highly concentrated amounts [9,10]. Urea could exist in as many as five polymorphs. UR is found in a tetragonal system crystal state, and its hexagonal system crystal state exists as a polymorphic form [11–14]. The hexagonal system of UR has been reported to improve solubility by forming co-crystals with small molecules such as palmitic acid in its opening [15].

CDs possess a ring structure formed by the α 1-4 glucoside bond of glucopyranose and are hydrophilic on the outside of the ring and near the edge, featuring a hydrophobic cavity [16–18]. Inclusion complexes are prepared by various methods, such as coprecipitation [19], lyophilization [20], and mixing and pulverization [21]. Furthermore, the formation of inclusion complexes can improve the solubility [22], stability [23], bioavailability [24], and controlled release [25] of the guest compound. The molecules that encapsulate other molecules, such as cyclodextrins, are referred to as hosts, and those that are encapsulated are referred to as guests. Due to this structure, CDs can encapsulate guest molecules, leading to the creation of inclusion complexes. The inclusion and complexation of hydrophobic compounds occur mainly through hydrophobic interactions between the cyclodextrin cavity walls and the guest molecules. In addition, other forces, such as dipole-dipole interactions and van der Waals, can be implicated in the guest binding. CDs can be used to incorporate non-polar molecules with a suitable dimension into the cavity, increasing their water solubility. A study has reported that coprecipitation causes oxethazaine and γ CD to form inclusion complexes, thus improving the dissolution of oxethazaine [26].

ASCP is stable in the presence of heat and light and retains the antioxidant and melanin inhibitory properties of its precursor, AA. ASCP has high preferential lipid solubility due to the presence of palmitic acid [7]. Urea and ASCP are used in dermatological products to promote hydration and prevent oxidative processes, respectively. The combination of these two molecules is thought to provide synergistic effects on skin. However, through the incorporation of hydrophobic groups in ascorbyl palmitate (ASCP), this ascorbic acid derivative becomes more lipophilic and less soluble with water, limiting the practicality of its applications [27,28]. Organic bases have been employed in the preparation of CD ternary complexes, but none has reported the incorporation of urea [29]. Complexes of ASCP and UR prepared using the evaporation method were found to improve the solubility of ASCP [30]. The improvement of solubility in aqueous solvents by the formation of inclusion complexes of ASCP and γ CD using the grinding mixture method has also been reported [31]. However, the feasibility of preparative methods (e.g., pulverization, evaporation) to combine ASCP and UR as an inclusion complex, which is important in dermatology, has not yet been attempted. Furthermore, the fusion mechanism of ASCP and UR into the γ CD cavity and the impact of ASCP/UR/ γ CD formulated ternary systems on the physicochemical properties of ASCP are not yet fully understood.

In this study, we prepared ASCP/UR complexes using our previously established preparation method and then compared them against a ternary complex of ASCP/UR with γ CD prepared by pulverization methods. Therefore, we prepared ternary complexes of ASCP/UR with γ CD to investigate changes in physicochemical properties such as thermal behavior and intermolecular activities, as well as to improve the solubility of ASCP/UR.

2. Materials and Methods

2.1. Materials

γ -Cyclodextrin (γ CD) was procured from Cyclochem Bio Co. (Kobe, Japan). Urea (UR) and ascorbyl palmitate (ASCP) were purchased from FUJIFILM Wako Pure Chemical Corporation (Osaka, Japan) and Tokyo Chemical Industry Co., Ltd. (Saitama, Japan), respectively

(Figure 1). Other chemicals were obtained from FUJIFILM Wako Pure Chemical Corporation.

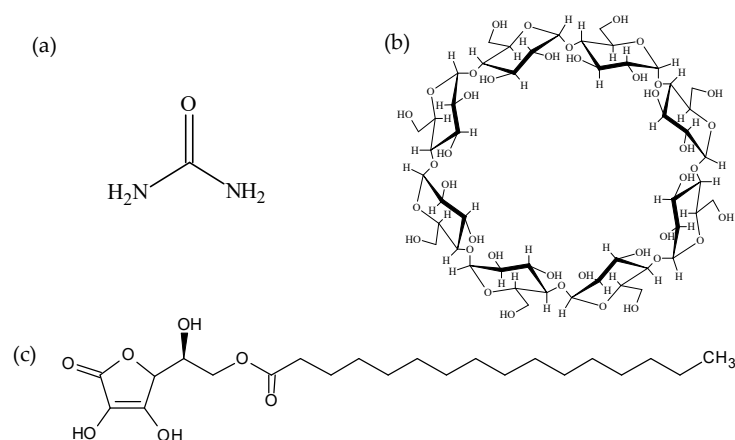


Figure 1. Chemical structures of (a) Urea (UR), (b) γ -Cyclodextrin (γ CD), (c) ASCP.

2.2. Preparation Methods

2.2.1. Preparation of Samples by Physical Mixture (PM)

A physical mixture (PM) was prepared by weighing AU (ASCP/UR) and γ CD at certain molar ratios (2/1, 1/1, 2/3, or 1/2) and then mixing with a vortex mixer for 1 min.

2.2.2. Preparation of Samples by the Evaporation Method

The sample was prepared by weighing ASCP and UR at a molar ratio of 1:12 and then mixing using a vortex mixer for 1 min. An evaporated sample (EVP) was prepared by exhaustive evaporation aided by a rotary evaporator. A PM (200 mg) composed of ASCP and UR was dissolved in 20 mL of methanol, the solvent was evaporated at 40 °C, and the resulting concentrated sample was centrifuged at 25 rpm to collect the formed crystals (EVP).

2.2.3. Preparation of Samples by Ground Mixture (GM)

Prepared EVP (ASCP/UR = 1/12) and γ CD at different molar ratios (2/1, 1/1, 2/3, or 1/2) were weighed to a total weight of 1 g, filled into an aluminum cell, and ground for 60 min using a vibrating rod mill (CMT TI-500ET, Fukushima, Japan).

2.3. Characterization Methods

2.3.1. Powder X-ray Diffraction (PXRD)

A powder X-ray diffractometer (Miniflex II, Rigaku Corporation, Tokyo, Japan) was utilized to perform the PXRD measurements. PXRD analysis was performed using Ni-filtered $\text{CuK}\alpha$ (30 kV, 15 mA) as the X-ray source. PXRD conditions were $2\theta = 5\text{--}40^\circ$ scan range at a scan rate of $4^\circ/\text{min}$. Each powder sample was spread uniformly on a glass plate prior to analysis.

2.3.2. Differential Scanning Calorimeter (DSC)

A high-sensitivity differential scanning calorimeter (Thermo Plus Evo, Rigaku Corporation, Tokyo, Japan) was utilized to investigate the thermal transitions of the samples and ternary complexes. Approximately 2 mg of the sample was placed and sealed in an aluminum pan and was subjected to an incremental heating rate of $5^\circ\text{C}/\text{min}$. The analysis was performed with flow rate of nitrogen gas at 60 mL/min.

2.3.3. Infrared (IR) Absorption Spectrum Measurement

The JASCO FT/IR-410 (Japan Spectroscopy Co., Ltd., Tokyo, Japan) was used to determine the IR absorption spectra using the KBr tablet method. The number of integration

times was 16 times, the resolution was 4 cm^{-1} , and the measurement wavenumber range was from 4000 to 400 cm^{-1} . Samples were mixed with potassium bromide (KBr) at a ratio of 1/20 (sample/KBr) by weight and compressed by manual pressing. Background correction was performed using compressed KBr alone.

2.3.4. Near Infrared (NIR) Spectroscopy

NIR spectroscopy measurements were performed using a NIR Flex N-500 spectrometer (Nippon Buchi). Each sample was placed in a sample holder, and the spectra were collected for 8 s in the range of $10,000$ – 4000 cm^{-1} at $25\text{ }^{\circ}\text{C}$ using a cell with a 1 mm optical path length.

2.3.5. ASCP Solubility Studies

ASCP was added with distilled water to a concentration of 0.1 mg/mL and shaken at 200 rpm for 1 h at $37\text{ }^{\circ}\text{C}$. After shaking, the resulting suspension was filtered through a $0.45\text{ }\mu\text{m}$ membrane filter. The filtrate was added to $200\text{ }\mu\text{L}$ of 1% DL-homocysteine and derivatized at $40\text{ }^{\circ}\text{C}$ for 15 min. An identical procedure was carried out for PM, EVP, and GM samples. Quantification of ASCP was performed using an HPLC system (Waters, Japan) at a wavelength of 266 nm equipped with an e2795 UV-Vis detector and a packed column ($5\text{ }\mu\text{m}$ diameter, $4.6\text{ mm ID} \times 250\text{ mm}$; Cosmosil 5C18-AR-II). The sample injection volume was $100\text{ }\mu\text{L}$ and the column temperature was maintained at $40\text{ }^{\circ}\text{C}$. The mobile phase was a mixture of methanol/acetic acid (85/15; pH 6.5), and the retention time of ASCP was approximately 10 min.

3. Results and Discussion

3.1. Investigation of Intermolecular Interaction in a Mixture of ASCP/UR = 1/12 and γCD

3.1.1. Powder X-ray Diffraction (PXRD) Measurement

Powder diffraction (PXRD) measurements were performed to investigate the crystalline state of the mixture of AU (ASCP/UR = 1/12) and γCD . PXRD patterns of ASCP, UR, EVP AU (ASCP/UR = 1/12), γCD , PM (AU (ASCP/UR = 1/12)/ γCD = 1/1, 1/2), and GM (AU (ASCP/UR = 1/12)/ γCD = 1/1, 1/2) are shown in Figure 2. It has been reported that the crystalline state of UR changes when it forms a complex with a drug [11]. In general, characteristic diffraction peaks of UR are observed at $2\theta = 22.0^{\circ}$ and 29.2° in its tetragonal system and at $2\theta = 22.9^{\circ}$ and 24.5° for URs in its hexagonal system. In PM (1/1) and PM (1/2), the characteristic γCD -derived peaks were observed at $2\theta = 6.0^{\circ}$ and 12.0° . In addition, characteristic peaks derived from EVP AU (ASCP/UR = 1/12) were observed at $2\theta = 23.0^{\circ}$ and 24.9° . In GM (1/1), new diffraction peaks were observed around $2\theta = 7.5^{\circ}$ and 16.6° , while characteristic peaks originating from EVP (ASCP/UR = 1/12) were observed at $2\theta = 23.4^{\circ}$ and 24.9° . On the other hand, a new diffraction peak at $2\theta = 7.4^{\circ}$ and 16.6° was observed in the GM (1/2) sample. These results indicate that the new diffraction peak identified in GM (1/2) is consistent with the tetragonal-columnar diffraction peak observed when γCD forms an inclusion complex [32]. The formation of inclusion complexes with CDs due to mechanochemical reactions such as crystallization, solid solution, and phase transition caused by mechanical energy such as friction and compression during the milling process of solid materials reported earlier is consistent with our observation [33,34]. It was inferred that AU (ASCP/UR = 1/12) formed an inclusion complex within the γCD cavity by these methods, resulting in a crystal structure different from that of EVP AU (ASCP/UR = 1/12).

3.1.2. Differential Scanning Calorimetry (DSC) Measurement

DSC measurements were performed to investigate the thermal properties of EVP AU (ASCP/UR = 1/12) and γCD (Figure 3). UR and the PM (ASCP/UR at a molar ratio of 1/12) had an endothermic peak due to UR at $131\text{ }^{\circ}\text{C}$ and $125\text{ }^{\circ}\text{C}$. It has been reported that the endothermic peak associated with the crystalline transition of UR from a tetragonal system to a hexagonal system can be observed at temperatures lower than the peak derived from the melting point of urea [30]. In the PM (AU/ γCD = 1/1, 1/2) and GM (AU/ γCD = 1/1),

an endothermic peak was observed at around 83 °C, which is attributed to the phase transition of urea from the hexagonal to the tetragonal system. An endothermic peak at 113.9 °C was also observed for EVP AU (ASCP/UR = 1/12). Interestingly, the characteristic phase transition-derived peak and the EVP (ASCP/UR = 1/12)-derived endothermic peak disappeared in GM (1/2). Generally, an emerging endothermic peak due to drug melting disappears when a drug is encapsulated in CD [30]. This suggests that the disappearance of the endothermic peak of AU (ASCP/UR = 1/12) in GM (AU/ γ CD = 1/2) may be due to the formation of an inclusion complex between ASCP/UR = 1/12 and γ CD. We have assumed that in the formed complex, the ratio between ACSP and UR must stay at 1/12. When the complex of ASCP and UR is dissociated by the ground mixing of AU (ASCP/UR = 1/12) and γ CD, the characteristic diffraction peaks of ASCP intact and UR intact should be observed by XRD. However, in GM (AU (ASCP/UR = 1/12)/ γ CD = 1/2), ASCP intact and UR intact were not confirmed. In addition, no UR-derived endothermic peak is observed in Figure 3h GM (AU (ASC/UR = 1/12)/ γ CD = 1/2) of the DSC measurement. Thus, we were satisfied that in GM (AU (ASCP/UR = 1/12)/ γ CD), the stoichiometric ratio of (ASCP/UR = 1/12) was ensured.

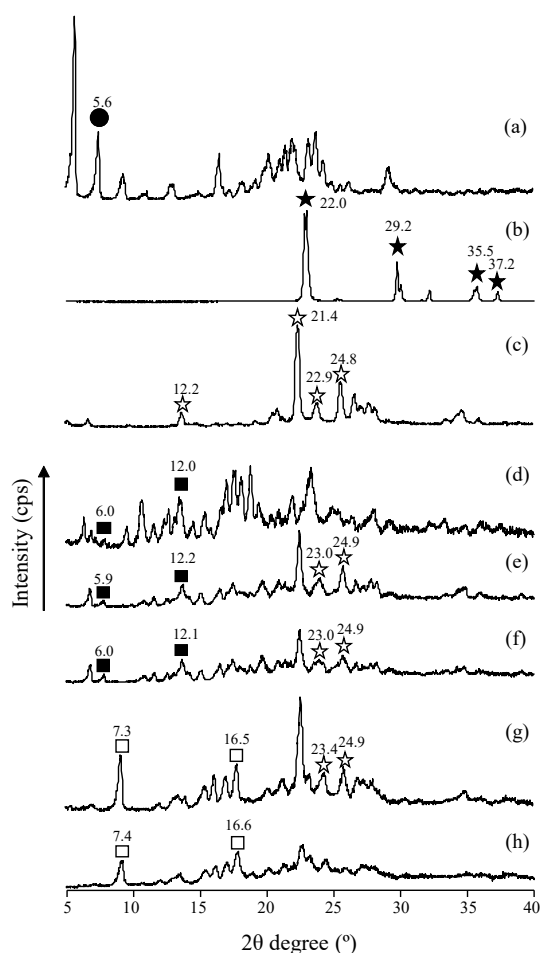


Figure 2. PXRD patterns of AU (ASCP/UR = 1/12)/ γ CD systems. (a) ASCP intact, (b) UR intact, (c) EVP AU (ASCP/UR = 1/12), (d) γ CD intact, (e) PM (AU (ASC/UR = 1/12)/ γ CD = 1/1), (f) PM (AU (ASC/UR = 1/12)/ γ CD = 1/2), (g) GM (AU (ASC/UR = 1/12)/ γ CD = 1/1), (h) GM (AU (ASC/UR = 1/12)/ γ CD = 1/2)●: ASCP, ★: UR (tetragonal form), ☆: UR (hexagonal form), ■: γ CD, □: γ CD (tetragonal-columnar form).

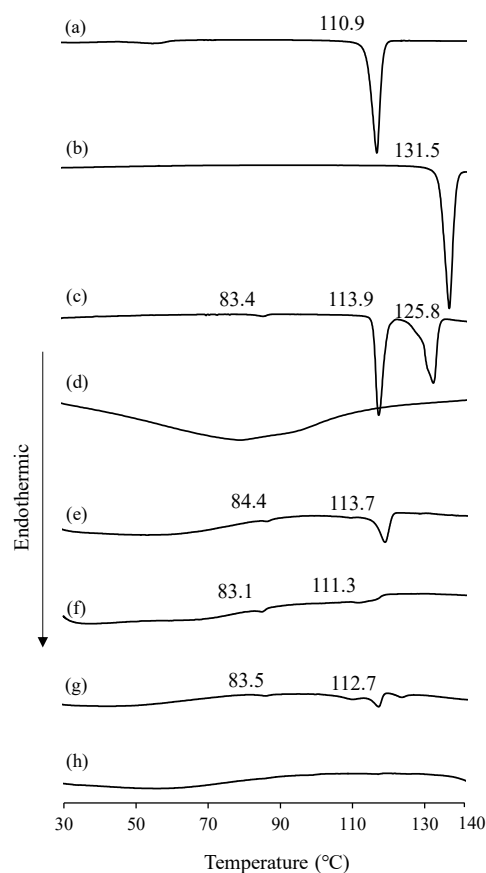


Figure 3. DSC curves of AU (ASCP/UR = 1/12)/ γ CD systems. (a) ASCP intact, (b) UR intact, (c) EVP AU (ASCP/UR = 1/12), (d) γ CD intact, (e) PM (AU (ASCP/UR = 1/12)/ γ CD = 1/1), (f) PM (AU (ASCP/UR = 1/12)/ γ CD = 1/2), (g) GM (AU (ASCP/UR = 1/12)/ γ CD = 1/1), (h) GM (AU (ASCP/UR = 1/12)/ γ CD = 1/2).

3.2. Inclusion of the Molar Ratio of ASCP/UR = 1/12 and γ CD

CDs display thermal behavior alterations such as the disappearance or shift of the melting point of the guest molecule due to the formation of inclusion complexes [35,36]. Molecular structure dynamic studies can help predict the decrease in entropy due to changes in the crystal structures of samples examined [37–39]. Therefore, calorimetric conversion by DSC measurement was performed to determine the optimum molar ratio of the complex. GM (2/1) had $-\Delta H = 58.7$ J/g, GM (1/1) had $-\Delta H = 19.5$ J/g, GM (2/3) had $-\Delta H = 11.0$ J/g, and GM (1/2) had $-\Delta H = 0.441$ J/g. GM (1/2) was found to be a thermally stable sample (Figure 4). From these results, it can be inferred that the sample with the highest thermal stability was GM (1/2), which is the optimum molar ratio, suggesting the possibility of an inclusion complex formation. It was apparent that decreasing the AU (ASCP/UR) γ CD molar ratio (2/1, 1/1, 2/3, or 1/2) resulted in increased thermal stability.

3.3. Examination of the Molecular State in the Solid State

The results of PXRD and DSC analyses suggested the formation of a complex from a mixture of milled materials with a molar ratio of AU (ASCP/UR = 1/12)/ γ CD = 1/2. We then performed infrared (IR) and near-infrared (NIR) absorption spectroscopy studies to investigate the molecular structure of the complex in its solid states.

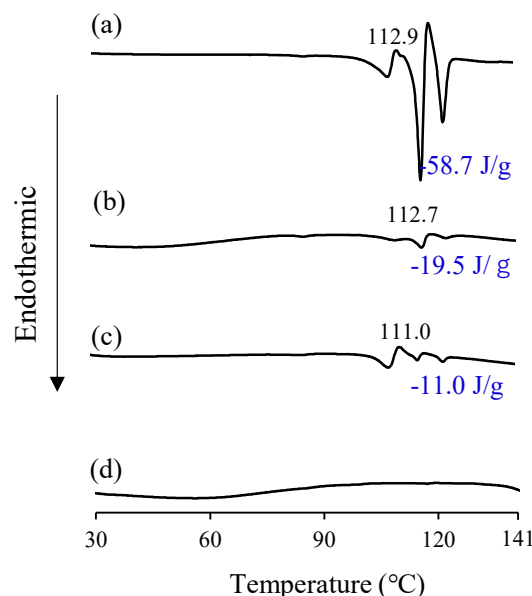


Figure 4. DSC curves of GM (AU (ASCP/UR)/ γ CD) systems. (a) GM (2/1), (b) GM (1/1), (c) GM (2/3), (d) GM (1/2).

3.3.1. Infrared (IR) Absorption Spectra

The IR spectra of ASCP, UR, γ CD, EVP AU (ASCP/UR = 1/12), PM (AU (ASCP/UR = 1/12)/ γ CD = 1/1), GM (AU (ASCP/UR = 1/12)/ γ CD = 1/1), PM (AU (ASCP/UR = 1/12)/ γ CD = 1/2), GM (AU (ASCP/UR = 1/12)/ γ CD = 1/2) are shown in Figure 5. In ASCP, a peak derived from the -CH group was observed at 2916 cm^{-1} . The C=O stretching peak of the palmitate side chain from ASCP was observed at 1730 cm^{-1} and the C=O stretching peaks of the lactone ring were observed at 1685 cm^{-1} and 1629 cm^{-1} (Figure 5a). In UR, C-N stretching peaks were observed at 1000 cm^{-1} , C=O group stretching peaks at 1672 cm^{-1} , and N-H stretching peaks at 3437 cm^{-1} , 3342 cm^{-1} , and 3286 cm^{-1} (Figure 5b). EVP AU (ASCP/UR = 1/12) exhibited shifting peaks originating from HN_2 vibrations, C-N stretching vibrations, C=O-based stretching vibrations, and N-H stretching vibrations of UR [31]. No significant peak shifts were observed in PM (AU (ASCP/UR)/ γ CD = 1/1, 1/2). On the other hand, in GM (AU (ASCP/UR)/ γ CD = 1/1), the N-H stretching vibration-derived peak from UR observed at 3396 cm^{-1} while at 3375 cm^{-1} in EVP AU (ASCP/UR = 1/12) shifted to 3412 cm^{-1} and 3342 cm^{-1} , while the peak at 3219 cm^{-1} did not shift (Figure 5c). The peak at 1016 cm^{-1} derived from the C-N stretching vibration of UR in EVP AU (ASCP/UR = 1/12) shifted to 1022 cm^{-1} . In addition, a peak at 1649 cm^{-1} derived from the C=O stretching vibration of EVP AU (ASCP/UR = 1/12), shifted to 1666 cm^{-1} and another peak that did not shift coexisted, suggesting that both the inclusion complex by γ CD and the EVP AU (ASCP/UR) complex were both present. Interestingly, in GM (AU (ASCP/UR)/ γ CD = 1/2), the N-H stretching vibration-derived peaks of UR in EVP (ASCP/UR = 1/12) were shifted to 3305 cm^{-1} and 3192 cm^{-1} , and the peak at 3219 cm^{-1} broadened. In EVP (ASCP/UR = 1/12), the C=O stretching peak of UR was shifted to 1656 cm^{-1} . (Figure 5h). The C-N stretching peak was shifted to 1020 cm^{-1} . These results suggest that in GM (AU (ASCP/UR)/ γ CD = 1/2), the N-H, C-N, and C=O groups in the molecular structure of UR, as well as the OH group from γ CD, are involved in hydrogen bonding in the formation of inclusion complexes.

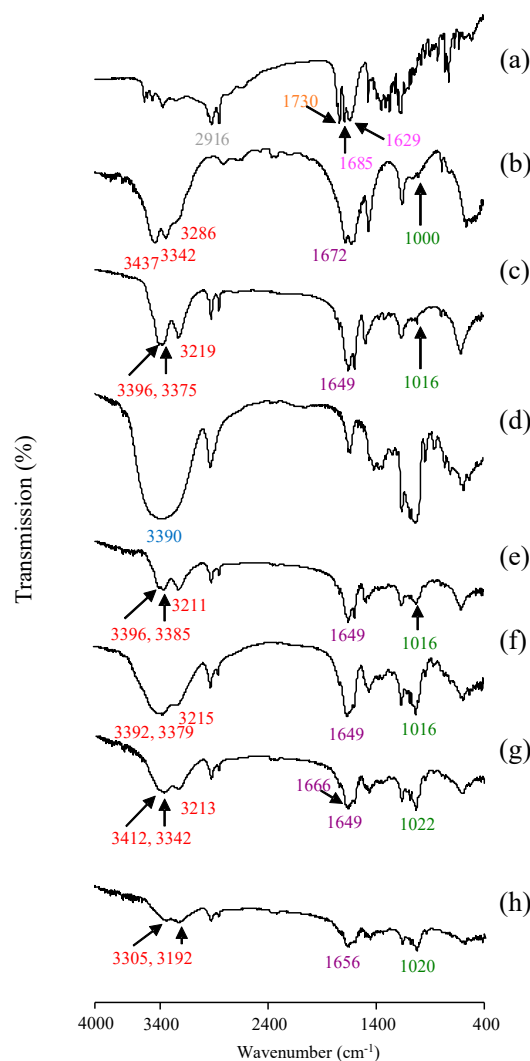


Figure 5. IR Spectra of AU (ASC/UR = 1/12)/ γ CD systems. (a) ASCP intact, (b) UR intact, (c) EVP AU (ASC/UR = 1/12), (d) γ CD intact, (e) PM (AU (ASC/UR = 1/12)/ γ CD = 1/1), (f) PM (AU (ASC/UR = 1/12)/ γ CD = 1/2), (g) GM (AU (ASC/UR = 1/12)/ γ CD = 1/1), (h) GM (AU (ASC/UR = 1/12)/ γ CD = 1/2).

3.3.2. Near-Infrared (NIR) Absorption Spectra

PXRD patterns and the results of DSC suggested that GM (AU (ASC/UR = 1/12)/ γ CD = 1/2) formed a complex. Although intermolecular interaction between the N-H, C-N, and C=O groups in the molecular structure of UR as well as the OH group from γ CD was speculated from FT-IR results, NIR measurement was performed because it was difficult to distinguish the -NH group from the -OH group. Thus, near-infrared (NIR) spectroscopy was performed in order to confirm the molecular interaction between ASCP, UR, and γ CD. The NIR spectra of ASCP, UR, EVP AU (ASC/UR = 1/12), γ CD, PM (AU (ASC/UR = 1/12)/ γ CD = 1/2), and GM (AU (ASC/UR = 1/12)/ γ CD = 1/2) are shown in Figure 6. In ASCP, the peaks derived from the CH group were observed at 5772 cm^{-1} and 5664 cm^{-1} (Figure 6b). In the AU (ASC/UR = 1/12)/ γ CD = 1/2, the peaks derived from the CH group of ASCP were observed at 5772 cm^{-1} and 5664 cm^{-1} , and similarly, in GM (1/2), the CH group of ASCP was observed at 5772 cm^{-1} and 5664 cm^{-1} [7]. In UR, NH-derived peaks were observed at 5000 cm^{-1} , 5120 cm^{-1} , and 5160 cm^{-1} . In EVP AU (ASC/UR = 1/12), the NH group-derived peaks in UR shifted to 5032 cm^{-1} and 5108 cm^{-1} and the peak at 5160 cm^{-1} of UR was broadened (Figure 6c). In the PM (AU (ASC/UR = 1/12)/ γ CD = 1/2), as well as in the EVP AU

(ASCP/UR = 1/12), the NH-derived peak of UR shifted to 5032 cm^{-1} and 5108 cm^{-1} , and the peak at 5160 cm^{-1} is broadened. In GM (AU (ASCP/UR = 1/12)/ γ CD = 1/2), the peak derived from the NH group of UR was broadened around 5072 cm^{-1} . A neat OH group of γ CD was observed at 7020 cm^{-1} (Figure 6a). In AU (ASCP/UR = 1/12)/ γ CD = 1/2), the OH group originating from γ CD was observed at 7020 cm^{-1} while the OH group derived from ASCP was observed at 7176 cm^{-1} . In GM (AU (ASCP/UR = 1/12)/ γ CD = 1/2), the peak at 7020 cm^{-1} derived from the OH group of γ CD was observed to shift to 7032 cm^{-1} [40,41]. The peak at 7176 cm^{-1} derived from the OH group of ASCP was observed to have broadened. From these results, it can be inferred that the CH group of ASCP is not responsible for the interaction, as no shift was observed in the peak derived from the CH group of ASCP in GM (AU (ASCP/UR = 1/12)/ γ CD = 1/2). The peak derived from the NH group of UR, which was shifted in EVP AU (ASCP/UR = 1/12), broadened in GM (AU (ASCP/UR = 1/12)/ γ CD = 1/2), and the peak derived from the OH group of γ CD also showed a shift.

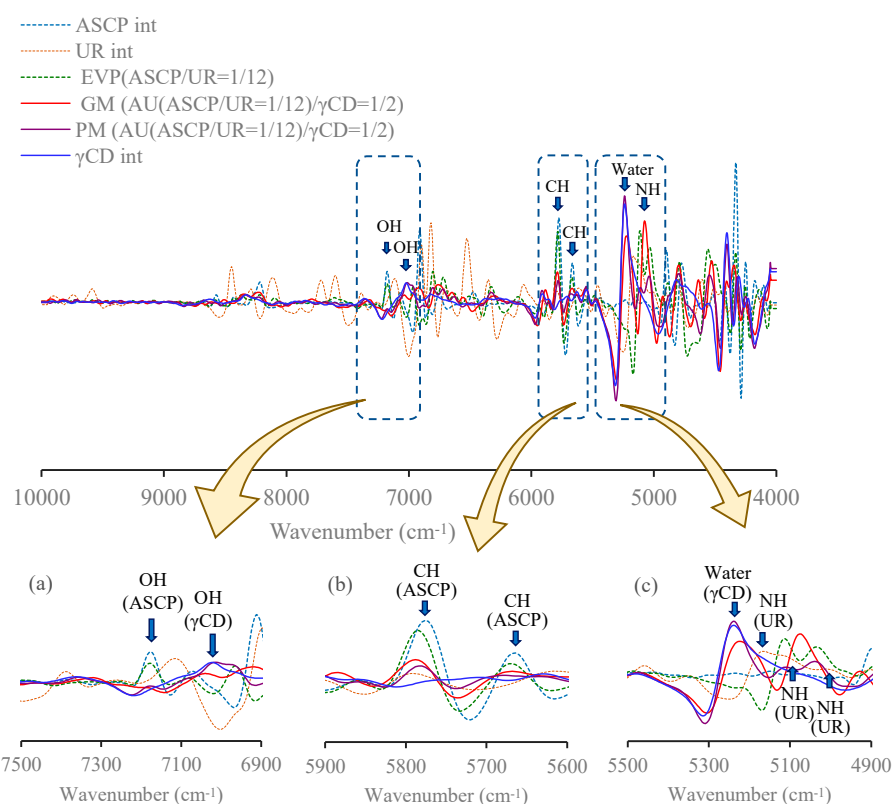


Figure 6. Second-derivative NIR absorption spectra for an AU (ASCP/UR = 1/12)/ γ CD system. (a) $7500\text{--}6900\text{ cm}^{-1}$, (b) $5900\text{--}5600\text{ cm}^{-1}$, (c) $5500\text{--}4900\text{ cm}^{-1}$.

These observations deduce that an interaction has occurred between the OH groups in the cavity of γ CD and the N-H group in UR. The broadening of the peak derived from the OH group of ASCP in GM (AU (ASCP/UR = 1/12)/ γ CD = 1/2) suggests that the OH group of γ CD in the neighboring complex interacts with the OH group attached to the lactone ring of ASCP, aiding in the formation of the three-component complex. These interactions suggest that AU (ASCP/UR) has been included within the cavity of γ CD.

3.4. Solubility Study of ASCP/UR = 1/12 and γ CD Complex

The results of solubility studies of ASCP, EVP (ASCP/UR = 1/12), PM (1/2), and GM (1/2) in distilled water are shown in Table 1. Preparative methods described in this study resulted in higher solubility of ASCP in distilled water despite no statistical significance. The solubility of ASCP is increased by 1.2-fold and 1.3-fold when prepared as

EVP and PM, respectively. Compared to ASCP alone, GM (1/2) improved the solubility of ASCP by approximately 1.9-fold and by approximately 1.6-fold when compared with EVP (ASCP/UR = 1/12). The solubility enhancement of GM (1/2) observed is related to the formation of an inclusion complex with γ CD. This finding may support the use of a similar strategy in formulating ASCP and UR formulations with enhanced skin permeation properties. However, the solubility was lower compared with the solubility of ASCP in GM (ASCP/ γ CD = 1/2) inclusion complex [26]. We hypothesize that in an aqueous solution, GM (1/2) may behave as a single entity of ASCP/UR = 1/12, liberated from its encapsulation in γ CD. In this study, we were surprised that the expected improvement in solubility was not achieved. Although we succeeded in preparing a three-component complex in this study, there was a minimal enhancement in solubility; nevertheless, the results were interesting from the viewpoint of drug–drug–CD molecular interactions in the solid state. Our results reveal the solubility enhancing effect of the UR and γ CD ternary-inclusion complexes on ASCP. The effects are considered limited, prompting an exploratory direction with other CDs (e.g., alpha, beta). Urea (UR) has moisturizing properties, hydrates the stratum corneum, has keratin cleavage properties, and is commonly used as a moisturizer, skin permeability enhancer, and solubilizer in pharmaceuticals and cosmetics [8,9]. UR is known to have a hydrotropic effect. Determination of UR degradation in aqueous solvent and appropriate pharmaceutical bases from a ternary-inclusion complex is also an imperative future direction of this research theme. The techniques used for encapsulating a hydrophilic molecule into a cyclodextrin-based metal-organic framework (CD-MOF) have been reported [42]. In the future, it will be interesting to try to adjust the complex using CD-MOF-1, which is derived from γ CD, as a new complex.

Table 1. Solubility of AU (ASCP/UR = 1/12)/ γ CD systems.

Samples	ASCP (μ g/mL)
ASCP intact	1.49 \pm 0.06
EVP AU (ASCP/UR = 1/12)	1.76 \pm 0.05
PM (AU (ASC/UR = 1/12)/ γ CD = 1/2)	1.95 \pm 0.14
GM (AU (ASC/UR = 1/12)/ γ CD = 1/2)	2.77 \pm 0.44
GM (ASCP/ γ CD) [26]	19.6 \pm 3.57

Results were expressed as mean \pm S.D. ($n = 3$) at 37 °C.

4. Conclusions

In this study, complexation between AU (ASCP/UR) and γ CD in the solid state using the mixed grinding method was revealed by PXRD, DSC, IR, and NIR spectroscopic measurements. AU (ASCP/UR)/ γ CD = 1/2 was confirmed to entrap the ASCP/UR complex within the cavity of γ CD. These results suggest that the inclusion complex is formed at the molar ratio (1/2) of AU (ASCP/UR = 1/12)/ γ CD by the ground mixture method. In this study, we focused on the physicochemical properties during complex formation. In the future, it would be interesting to evaluate the antioxidant test and melanogenesis inhibitory ability of ASCP as indicators of its functionality in the skin.

Author Contributions: Conceptualization, Y.I., A.N., F.J.A. and G.L.S.; methodology, Y.I., A.N., F.J.A. and G.L.S.; software, Y.I., A.N., T.T., T.Y. and M.K.; validation, Y.I., A.N., T.T., T.Y. and M.K.; formal analysis, Y.I., A.N., F.J.A., G.L.S., T.T., T.Y. and M.K.; investigation, Y.I., A.N., T.T., T.Y. and M.K.; resources, Y.I., A.N., T.T., T.Y. and M.K.; data curation, Y.I., A.N., T.T., T.Y. and M.K.; writing—original draft preparation, Y.I., A.N., F.J.A. and G.L.S.; writing—review and editing, Y.I., A.N., F.J.A. and G.L.S.; visualization, Y.I., A.N., F.J.A. and G.L.S.; supervision, Y.I., A.N., T.T. and T.Y.; project administration, Y.I., A.N., T.T. and T.Y.; funding acquisition, Y.I., A.N., T.T. and T.Y. All authors have read and agreed to the published version of the manuscript.

Funding: This research received no external funding.

Institutional Review Board Statement: Not applicable.

Informed Consent Statement: Informed consent was obtained from all subjects involved in the study.

Data Availability Statement: Not applicable.

Acknowledgments: The authors wish to thank Cyclo Chem Co., Ltd. (for providing γ CD), and Tarumi at Buchi Labortechnik AG (for assisting with NIR spectroscopy). The authors wish to thank Junki Tomita (Instrument Analysis Center, Josai University) for his helpful advice regarding PXRD, DSC measurements. We also acknowledge the members of the Laboratory of Nutri-Pharmacotherapeutics Management for their assistance in conducting the experiments.

Conflicts of Interest: The authors declare no conflict of interest.

References

1. Niki, E.; Saito, T.; Kawakami, A.; Kamiya, Y. Inhibition of oxidation of methyl linoleate in solution by vitamin E and vitamin C. *J. Biol. Chem.* **1984**, *259*, 4177–4182. [[CrossRef](#)] [[PubMed](#)]
2. Telang, P.S. Vitamin C in dermatology. *Ind. Dermatol. Online J.* **2013**, *4*, 143–146. [[CrossRef](#)] [[PubMed](#)]
3. Liston, L.S.; Rivas, P.L.; Sakdiset, P.; See, G.L.; Arce, F.A.J. Chemical permeation enhancers for topically-applied vitamin C and its derivatives: A systematic review. *Cosmetics* **2022**, *9*, 85. [[CrossRef](#)]
4. Ahmad, I.; Sheraz, M.A.; Ahmed, S.; Shaikh, R.H.; Vaid, F.H.; ur Khattak, R.S.; Ansari, S.A. Photostability and interaction of ascorbic acid in cream formulations. *AAPS PharmSciTech* **2011**, *12*, 917–923. [[CrossRef](#)]
5. Ochiai, Y.; Kaburagi, S.; Obayashi, K.; Ujiie, N.; Hashimoto, S.; Okano, Y.; Masaki, H.; Ichihashi, M.; Sakurai, H. A new lipophilic pro-vitamin C, tetra-isopalmitoyl ascorbic acid (VC-IP), prevents UV-induced skin pigmentation through its anti-oxidative properties. *J. Dermatol. Sci.* **2006**, *44*, 37–44. [[CrossRef](#)]
6. Huang, W.Y.; Lee, P.C.; Huang, L.K.; Lu, L.P.; Liao, W.C. Stability studies of ascorbic acid 2-glucoside in cosmetic lotion using surface response methodology. *Bioorg. Med. Chem. Lett.* **2013**, *23*, 1583–1587. [[CrossRef](#)]
7. Segall, A.I.; Moyano, M.A. Stability of vitamin C derivatives in topical formulations containing lipoic acid, vitamins A and E. *Int. J. Cosmet. Sci.* **2008**, *30*, 453–458. [[CrossRef](#)]
8. Trommer, H.; Neubert, R.H.H. Overcoming the stratum corneum: The modulation of skin penetration. *Skin Pharmacol. Physiol.* **2006**, *19*, 106–121. [[CrossRef](#)]
9. Mueller, J.; Oliverira, J.S.; Barker, R.; Trapp, M.; Schroeter, A.; Brezesinski, G.; Neubert, R.H. The effect of urea and taurine as hydrophilic penetration enhancers on stratum corneum lipid models. *Biochim. Biophys. Acta* **2016**, *1858*, 2006–2018. [[CrossRef](#)]
10. Sakurai, H.; Suzuki, M.; Itakura, S.; Todo, H.; Arce, F., Jr.; See, G.L.; Tanikawa, T.; Inoue, Y. Preparation, Characterization, Solubility, and Antioxidant Capacity of Ellagic Acid-Urea Complex. *Materials* **2022**, *15*, 2836. [[CrossRef](#)]
11. Lamelas, F.J.; Dreger, Z.A.; Gupta, Y.M. Raman and X-ray scattering studies of high-pressure phases of urea. *J. Phys. Chem. B* **2005**, *109*, 8206–8215. [[CrossRef](#)]
12. Olejniczak, A.; Ostrowska, K.; Katrusiak, A. H-bond breaking in high-pressure urea. *J. Phys. Chem. C* **2009**, *113*, 15761–15767. [[CrossRef](#)]
13. Dziubek, K.; Citroni, M.; Fanetti, S.; Cairns, A.B.; Bini, R. High-pressure high-temperature structural properties of urea. *J. Phys. Chem. C* **2017**, *121*, 2380–2387. [[CrossRef](#)]
14. Dhall, M.; Madan, A.K. Studies on urea co-inclusion complexes of simvastatin for improvement of pharmaceutical characteristics. *J. Incl. Phenom. Macrocycl. Chem.* **2015**, *81*, 105–120. [[CrossRef](#)]
15. White, M.A. Origins of thermodynamic stability of urea: Alkane inclusion compounds. *Can. J. Chem.* **1998**, *76*, 1695–1698. [[CrossRef](#)]
16. Arima, H.; Motoyama, K.; Higashi, T. Potential Use of Cyclodextrins as Drug Carriers and Active Pharmaceutical Ingredients. *Chem. Pharm. Bull.* **2017**, *65*, 341–348. [[CrossRef](#)]
17. Chao, J.; Wang, H.; Zhao, W. Investigation of the inclusion behavior of chlorogenic acid with hydroxypropyl- β cyclodextrin. *Int. J. Biol. Macromol.* **2012**, *50*, 277–282. [[CrossRef](#)]
18. Pápay, Z.E.; Sebestyén, Z.; Ludányi, K.; Kállai, N.; Balogh, E.; Kósa, A.; Somavarapu, S.; Böddi, B.; Antal, I. Comparative evaluation of the effect of cyclodextrins and pH on aqueous solubility of apigenin. *J. Pharm. Biomed. Anal.* **2016**, *117*, 210–216. [[CrossRef](#)]
19. Anselmi, C.; Centini, M.; Ricci, M.; Buonocore, A.; Granata, P.; Tsuno, T.; Facino, R.M. Analytical characterization of a ferulic acid/ γ -cyclodextrin inclusion complex. *J. Pharm. Biomed. Anal.* **2006**, *40*, 875–881. [[CrossRef](#)]
20. Zoppi, A.; Delrivo, A.; Aiassa, V.; Longhi, M.R. Binding of Sulfamethazine to β -cyclodextrin and Methyl- β -cyclodextrin. *AAPS PharmSciTech* **2013**, *14*, 727–735. [[CrossRef](#)]
21. Aigner, Z.; Berkesi, O.; Farkas, G.; Szabó-Révész, P. DSC, X-ray and FT-IR studies of a gemfibrozil/dimethyl- β -cyclodextrin inclusion complex produced by co-grinding. *J. Pharm. Biomed. Anal.* **2011**, *57*, 62–67. [[CrossRef](#)] [[PubMed](#)]
22. Zhang, Q.F.; Nie, H.C.; Shangguang, X.C.; Yin, Z.P.; Zheng, G.D.; Chen, J.G. Aqueous Solubility and Stability Enhancement of Astilbin through Complexation with Cyclodextrins. *J. Agric. Food Chem.* **2012**, *61*, 151–156. [[CrossRef](#)] [[PubMed](#)]
23. Zhang, S.X.; Fan, M.G.; Liu, Y.Y.; Ma, Y.; Zhang, G.J.; Yao, J.N. Inclusion complex of spironaphthoxazine with γ -cyclodextrin and its photochromism study. *Langmuir* **2007**, *23*, 9443–9446. [[CrossRef](#)] [[PubMed](#)]

24. Miyoshi, N.; Wakao, Y.; Tomono, S.; Tatemichi, M.; Yano, T.; Ohshima, H. The enhancement of the oral bioavailability of γ -tocotrienol in mice by γ -cyclodextrin inclusion. *J. Nutr. Biochem.* **2011**, *22*, 1121–1126. [[CrossRef](#)] [[PubMed](#)]
25. Martin, A.; Tabary, N.; Leclercq, L.; Junthip, J.; Degoutin, S.; Aubert-Viard, F.; Cazaux, F.; Lyskawa, J.; Janus, L.; Bria, M.; et al. Multilayered textile coating based on a β -cyclodextrin polyelectrolyte for the controlled release of drugs. *Carbohydr. Polym.* **2012**, *93*, 718–730. [[CrossRef](#)]
26. Inoue, Y.; Suzuki, R.; Horage, M.; Togano, M.; Kimura, M.; Ogihara, M.; Ando, S.; Kikuchi, J.; Murata, I.; Kanamoto, I. Effects of oxethazaine and gamma-cyclodextrin complex formation on intestinal contractions. *World J. Pharm. Sci.* **2016**, *4*, 269–280.
27. Saokham, P.; Burapapadh, K.; Praphanwittaya, P.; Loftsson, T. Characterization and Evaluation of Ternary Complexes of Ascorbic Acid with γ -Cyclodextrin and Poly(vinyl Alcohol). *Int. J. Mol. Sci.* **2020**, *21*, 4399. [[CrossRef](#)]
28. Hu, X.; Wei, B.; Li, H.; Wu, C.; Bai, Y.; Xu, X.; Jin, Z.; Tian, Y. Preparation of the β -cyclodextrin-vitamin C (β -CD-Vc) inclusion complex under high hydrostatic pressure (HHP). *Carbohydr. Polym.* **2012**, *90*, 1193–1196. [[CrossRef](#)]
29. Aiassa, V.; Garnero, C.; Longhi, M.R.; Zoppi, A. Cyclodextrin Multicomponent Complexes: Pharmaceutical Applications. *Pharmaceutics* **2021**, *13*, 1099. [[CrossRef](#)]
30. Inoue, Y.; Niiyama, D.; Murata, I.; Kanamoto, I. Usefulness of Urea as a Means of Improving the Solubility of Poorly Water-Soluble Ascorbyl Palmitate. *Int. J. Med. Chem.* **2017**, *2017*, 4391078. [[CrossRef](#)]
31. Inoue, Y.; Horage, M.; Suzuki, R.; Niiyama, D.; Urano, R.; Ando, S.; Kikuchi, J.; Murata, I.; Kanamoto, I. Study on Complexation of Ascorbic Acid Derivatives With γ -Cyclodextrin. *Int. J. Pharm.* **2017**, *7*, 9–21.
32. Higashi, K.; Ideura, S.; Waraya, H.; Limwikrant, W.; Moribe, K.; Yamamoto, K. Simultaneous Dissolution of Naproxen and Flurbiprofen from a Novel Ternary γ -Cyclodextrin Complex. *Chem. Pharm. Bull.* **2010**, *58*, 769–772. [[CrossRef](#)]
33. Ikeda, A.; Ishikawa, M.; Aono, R.; Kikuchi, J.; Akiyama, M.; Shinoda, W. Regioselective Recognition of a [60] Fullerene-Bisadduct by Cyclodextrin. *J. Org. Chem.* **2013**, *78*, 2534–2541. [[CrossRef](#)]
34. Xie, J.; Yang, F.; Shi, X.; Zhu, X.; Su, W.; Wang, P. Improvement in solubility and bioavailability of puerarin by mechanochemical preparation. *Drug Dev. Ind. Pharm.* **2013**, *39*, 826–835. [[CrossRef](#)]
35. Iwata, M.; Fukami, T.; Kawashima, D.; Sakai, M.; Furuishi, T.; Suzuki, T.; Tomono, K.; Ueda, H. Effectiveness of mechanochemical treatment with cyclodextrins on increasing solubility of glimepiride. *Die Pharm. Int. J. Pharm. Sci.* **2009**, *64*, 390–394.
36. Suzuki, R.; Inoue, Y.; Tsunoda, Y.; Murata, I.; Isshiki, Y.; Kondo, S.; Kanamoto, I. Effect of γ -cyclodextrin derivative complexation on the physicochemical properties and antimicrobial activity of hinokitiol. *J. Incl. Phenom. Macrocycl. Chem.* **2015**, *83*, 177–186. [[CrossRef](#)]
37. Kitamura, S.; Isuda, H.; Shimada, J.; Takada, T.; Takaha, T.; Okada, S.; Mimura, M.; Kajiwara, K. Conformation of cyclomaltooligosaccharide (“cycloamylose”) of dp21 in aqueous solution. *Carbohydr. Res.* **1997**, *304*, 303–314. [[CrossRef](#)]
38. Kitamura, S. Cyclic Oligosaccharides and Polysaccharides. In *Cyclic Polymers*, 2nd ed.; Semlyen, J.A., Ed.; Kluwer Academic Publishers: Dordrecht, The Netherlands, 2000; Chapter 4; pp. 125–160.
39. Shimada, J.; Handa, S.; Kaneko, H.; Takada, T. Conformation of Novel Cycloamylose: Topological Aspects and Simulations. *Macromolecules* **1996**, *29*, 6408–6421. [[CrossRef](#)]
40. Lestander, T.A.; Rudolfsson, M.; Pommer, L.; Nordin, A. NIR provides excellent predictions of properties of biocoal from torrefaction and pyrolysis of biomass. *Green Chem.* **2014**, *16*, 4906–4913. [[CrossRef](#)]
41. Gaydou, V.; Kister, J.; Dupuy, N. Evaluation of multiblock NIR/MIR PLS predictive models to detect adulteration of diesel/biodiesel blends by vegetal oil. *Chemom. Intell. Lab. Syst.* **2011**, *106*, 190–197. [[CrossRef](#)]
42. Inoue, Y.; Nanri, A.; Murata, I.; Kanamoto, I. Characterization of Inclusion Complex of Coenzyme Q10 with the New Carrier CD-MOF-1 Prepared by Solvent Evaporation. *AAPS PharmSciTech* **2018**, *19*, 3048–3056. [[CrossRef](#)] [[PubMed](#)]

Disclaimer/Publisher’s Note: The statements, opinions and data contained in all publications are solely those of the individual author(s) and contributor(s) and not of MDPI and/or the editor(s). MDPI and/or the editor(s) disclaim responsibility for any injury to people or property resulting from any ideas, methods, instructions or products referred to in the content.